Journal of the Taiwan Institute of Chemical Engineers 71 (2017) 265–276

Contents lists available at ScienceDirect

Journal of the Taiwan Institute of Chemical Engineers

journal homepage: www.elsevier.com/locate/jtice

Separation of oil/water emulsion using a new PSf/pebax/F-MWCNT nanocomposite membrane

Javad Saadati, Majid Pakizeh*

Department of Chemical Engineering, Faculty of Engineering, Ferdowsi University of Mashhad, P.O. Box: 9177948974, Mashhad, Iran

ARTICLE INFO

Article history:
Received 26 July 2016
Revised 13 November 2016
Accepted 17 December 2016
Available online 29 December 2016

Keywords:
Wastewater treatment
Nanofiltration
Oil/water emulsion
Pebax 2533

ABSTRACT

In this study a new PSf/pebax/F-MWCNTs nanocomposite membrane was prepared, characterized and used for nanofiltration of oil/water emulsion. For this purpose, the porous PSf support was prepared and then a thin layer of pebax as selective layer was coated on it. The effect of adding 0.5, 1 and 2 wt% of functionalized multiwall carbon nanotubes (F-MWCNTs) on the morphology and separation properties of resulting membranes were studied systematically. Prepared membranes were analyzed using SEM, FTIR, contact angel, tensile strength and TGA analyses. FTIR results approved the stabilization of F-MWCNTs in membrane matrix. SEM showed the membrane surface was defect free and F-MWCNTs particles were not agglomerated. Increasing F-MWCNT up to 2 wt%, increased hydrophilicity, tensile strength and thermal stability. Separation of oil/water emulsion was investigated at pressure range of 10–20 bar The highest permeate flux was obtained for 0.5 wt% F-MWCNTs loading while the sample containing 2.0 wt% F-MWCNTs showed the best oil rejection at all studied pressures. Results revealed that oil rejection was decreased with pressure. Finally, flux recovery, irreversible and reversible fouling was analyzed for all the prepared membranes at all pressures.

1. Introduction

Oil-in-water emulsions are common wastewater streams of many types of industrial units, such as the food industry. Many of these solutions contain over 10% oil which is chemically emulsified into the water phase because of the existence of surfactants in environment. The entire mixture, even though it contains less than 10% total oil, cannot be discharged to environment. In most localities, this waste fluid should be drained as hazardous waste. Treatment of oily wastewaters is performed by a variety of methods including gravity and centrifugal separations, chemical treatment, flotation, filtration, membrane processes, evaporation, activated carbon adsorption, porous silicone sponge and biological methods [1–4]. Among these techniques, membrane separation can be used to remove most of the water from the emulsion and consequently reduce the volume of oil-containing solutions.

Traditional ultrafiltration technology has provided for relatively clean water that was once suitable for sewer discharge but generally inadequate for reuse. However, recent changes in sewer discharge limits have created a need to produce even cleaner water, with an emphasis on reuse. In many locations, ultrafiltration treatment alone does not meet environmental discharge laws. Some companies have resorted to secondary treatment steps in order to comply with the tightening regulations. A related type of membrane technology, nanofiltration (NF), may offer a cost-effective means of separating recyclable or sewerable water from oil [5].

NF has a very appropriate capability to serve in waste recovery applications like oil/water separation. The NF permeate from oily solutions is cleaner than the UF permeate, therefore it gives more opportunity for in-house recycle. If discharge is favored, NF permeate can also be clean enough to meet tightening discharge requirements [6].

Chan et al. [7] studied nanofiltration of oily wastewater using PASA membranes and found that the PASA NF membranes were effective in removing oil from oily wastewater, under an operating pressure of 2–3 psi, a constant flux of 5 $L\,m^2\,h^{-1}$ and 99.6% retention of a solution of 5000 ppm olive oil could be achieved. Sadeghian et al. [8] used a γ-Al_2O_3 nanofiltration membrane to eliminate oily hydrocarbon contaminants from wastewater and the removal efficiency higher than 90% was obtained. Panpanit et al. [6] investigated the potentials of polysulfone and cellulose acetate UF and NF membrane for separation of oil water emulsion generated from car washing operations which consists of lubricant oil with distilled water and anionic emulsifier. Results indicated that the NF membrane produced higher TOC removal and less fouling than UF. It is because the NF membrane exhibits a moderate to strong anionic surface charge. For this reason, the surface of the

* Corresponding author.

http://dx.doi.org/10.1016/j.jtice.2016.12.024
1876-1070/

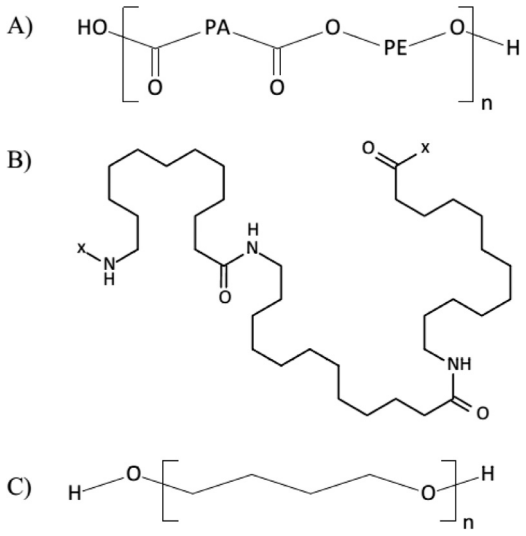

Fig. 1. Molecular structures of pebax and components of pebax 2533: (A) pebax, (B) polyamide (nylon 12) and (C) poly(tetramethylene oxide) (ether).

membrane will repel the anionic emulsifier. Therefore, membrane flux is not decreased significantly due to less adsorption of the emulsifier on the membrane surface. Chakrabarty et al. [9] studied cross flow ultrafiltration of stable oil-in-water emulsion using polysulfone membranes and found that fouling degree varied with membrane characteristics. Yu et al. [10] in another study used a tubular UF module equipped with PVDF membranes modified by inorganic nano-sized alumina particles to purify oily wastewater from an oil field. They found that the addition of nano-sized alumina particles improved membrane antifouling performance.

Pebax is a group of copolymers including hard polyamide (PA) segments and soft polyether (PE) segments as demonstrated in Fig. 1. In pebax molecules, PA segments promote mechanical strength while PE segments provide good affinity to organic solvents. Depending on the nature and proportion of PA and PE segments, the characteristics of the pebax polymer can be varied. In general, when the proportion of the flexible PE segment is higher, the pebax polymer is more organophillic.

Carbon nanotubes (CNTs) as nanofiller in polymer matrix have attracted a great deal of attention because of their high specific surface area, easy functionalization, chemical stability and proper compatibility. CNTs are also one of the candidates to create a surface with a roughness at micro/nanometer level due to their rigid cylindrical nanostructures with a diameter ranging from about 1 nm to dozens of nanometers and length ranging from hundreds of nanometers to micrometers, which could lead to the increase of efficient filtration area and permeability of the composite membranes [11]. In some literatures, the increments in specific parameters like hydrophilicity, permeability and rejection have been studied because of adding CNTs to polymeric membranes [12–14].

However, to the best of our knowledge, the preparation of nanocomposite membrane including PSf support membrane and modified pebax 2533 selective layer by F-MWCNT and its application in separation of O/W emulsion has not been previously investigated.

In this study, PSf/pebax composite membranes with different loadings of F-MWCNTs were prepared, characterized and used in separation of O/W emulsion. The porous support membrane was fabricated from PSf and F-MWCNTs were used in the pebax top selective layer. FTIR was used to characterize functionalized MWCNTs. The prepared membranes were characterized using SEM, FTIR, TGA, mechanical strength and contact angle tests. The permeation and oil fouling-resistant property were extensively investigated using a cross-flow NF experimental setup. Furthermore, the flux recovery of membranes, the efficiency of membrane washing and the effect of pressure on permeate flux and oil rejection were examined and analyzed.

2. Materials and methods

2.1. Chemicals

Poly(sulfone) (PSf) used to prepare the ultra porous substrate was purchased from Sigma–Aldrich. Pebax 2533 was purchased from Arkema, France. N-methylpyrrolidone (NMP) and isobutanol as solvent with analytical grade were supplied by Merck. Deionized water for the preparation of feed solutions was supplied from membrane laboratory. The functionalized MWCNTs (diameter$<$ 30 nm, length of 5–15 μm and purity$>$ 95%) were purchased from Nanotechnology Lab, Iran. Tween-20 as an emulsifier was supplied from Merck. Corn oil was purchased from a local grocery store.

2.2. Preparation of composite membrane

Composite membranes of pebax were prepared on PSf ultrafiltration substrate by solution casting and solvent evaporation technique. Ultra-porous PSf substrate was prepared by the phase inversion technique from a 12% (w/v) solution of the polymer in NMP solvent. The film was cast onto a woven polyester fabric using a casting bar (Neurtek 2,281,205, Spain) and immersed in a water bath for 24 h For pebax 2533, a bubble-free solution of 12% (w/v) of the polymer in isobutanol was prepared at 90 °C and casted on PSf substrate to the desired thickness using a hand-made adjustable casting bar. Solvent was evaporated in an oven at 60 °C for 10 min to obtain PSf/pebax composite membrane. For preparation of nanocomposite membranes, pebax polymer was added after adequate dispersing of F-MWCNTs in solvent using an ultrasound bath. About 30 min of sonication was enough to obtain a well dispersed mixture. Casting solution composition for all prepared membranes is presented in Table 1.

2.3. Preparation of the emulsions

The oil–water emulsion consisted of corn oil, Tween-20 and distilled water. After weighting, oil and surfactant with mass ratio of 3/1 were added to the distilled water. The emulsion was generated using a blender (Ultra Turrax model T25, Janke & Kunkel GmbH, Staufen, Germany) by mixing for 5 min at a high speed.

2.4. Membrane characterization

In order to identify the membrane structure, various characterization analyses consisted of FTIR, SEM, TGA, mechanical strength test and water contact angle were performed on prepared membranes. Each test will be discussed in more detail in the following sections.

2.4.1. Fourier transform infrared spectroscopy (FTIR)

FTIR (Thermo Nicolet Avatar 370) was used to characterize presence of functional groups in the F-MWCNTs and verifying formation of polymer modified F-MWCNTs.

2.4.2. Scanning electron microscopy (SEM)

The surface and cross section of membranes were examined by using a scanning electron microscope (SEM). The samples of the membranes were frozen in liquid nitrogen and fractured. After sputtering with gold, they were viewed with a Cam Scan SEM model Kykem3200 microscope.

Table 1
Name and casting solution composition for all prepared membranes.

Sample code	Selective layer		
	pebax 2533 (wt%)	n-butanol (wt%)	F-MWCNT (wt%)
PSf/pebax	12	88	0
PSf/pebax/0.5%F-MWCNT	11.94	88	0.06
PSf/pebax/1%F-MWCNT	11.88	88	0.12
PSf/pebax/2%F-MWCNT	11.76	88	0.24

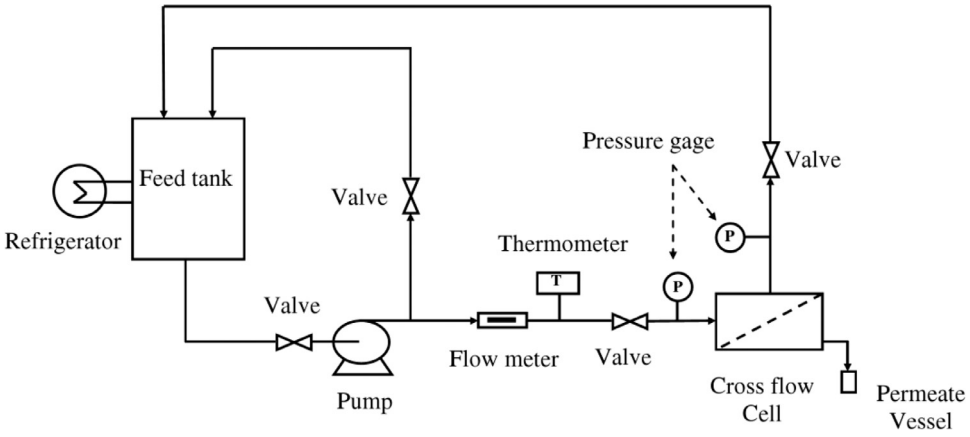

Fig. 2. Scheme of nanofiltration set up.

2.4.3. Thermogravimetric analysis (TGA)

Thermogravimetric analyses (TGA) of both of the PSf/pebax membrane and PSf/pebax/F-MWCNTs nanocomposite membrane were carried out using TGA-50 Shimadzu. Samples were heated in air from room temperature to 850 °C at a heating rate of 10 °C/min.

2.4.4. Mechanical strength test

The tensile strength at break of the nanocomposite membranes were measured using a universal testing machine (ZWICK-Z250, Germany), by employing a deformation speed of 5 mm/min at room temperature. Three membranes of each case were tested and the average tensile strengths were reported.

2.4.5. Water contact angle test

The static contact angles were measured with a contact angle measuring instrument (OCA15plus, Dataphysics, Germany). Deionized water was used as the probe liquid in all measurements and the contact angles between water and the membrane surface were measured for the evaluation of the membrane hydrophilicity. To minimize the experimental error, the contact angle was measured at three random locations for each sample and the average was reported.

2.4.6. Nanofiltration experiments

A cross-flow system as shown in Fig. 2 was employed for nanofiltration experiments. The 316 L stainless steel cell had an effective membrane area of 9.62 cm^2. To determine permeate flux, the permeate samples were collected after 1 h of operation. The permeate flux, J ($L/(m^2\,h)$) was calculated using the following equation:

$$J = \frac{V}{A.t} \tag{1}$$

Where V (L) is the volume of permeate, A (m^2) is the effective membrane surface area and t (h) is the permeate collection time. Concentrations of the feed and permeate were analyzed using an ultraviolet spectrophotometer (UV-VIS 6320D, England) at the wavelength of 243.4 nm. Under the preset separation pressure and apparent flow rate, the permeate flux and operation time were recorded regularly until the permeate flux reached a relatively constant value. Each run of experiments was repeated at least three times to ensure a duplicable result. The oil rejection efficiency is calculated according to following expression:

$$R(\%) = \left[1 - \left(\frac{\%\ \text{Oil in permeate}}{\%\ \text{Oil in feed}}\right)\right] \times 100 \tag{2}$$

2.4.7. Analysis of membrane fouling

After filtration of O/W emulsion, the membranes were washed with distilled water. The membranes were initially rinsed and then were immersed in distilled water for 20 min. This was followed by evaluation of water flux of cleaned membranes J_{W2} ($L/m^2\,h$). The flux recovery ratio (*FRR*) was calculated as follow:

$$FRR = \frac{J_{W2}}{J_{W1}} \times 100 \tag{3}$$

where J_{W1} ($L\,m{-}^2\,h$) is pure water flux before filtration of O/W emulsion.

Generally, higher *FRR* implies better antifouling property of the nanofiltration membrane. To analyze the fouling process in details, several ratios were defined to describe the fouling resistance of the prepared membranes. Reversible fouling ratio (R_r) and irreversible fouling ratio (R_{ir}) were also defined and calculated by following equations:

$$R_r = \frac{J_{W2} - J_P}{J_{W1}} \times 100 \tag{4}$$

$$R_{ir} = \frac{J_{W1} - J_{W2}}{J_{W1}} \times 100 \tag{5}$$

where J_p ($L/m^2\,h$) is permeate flux.

3. Results and discussion

3.1. Characterization of F-MWCNTs

FTIR was used to recognize introduced functional groups onto the surface of modified MWCNT. A difference between FTIR spectra

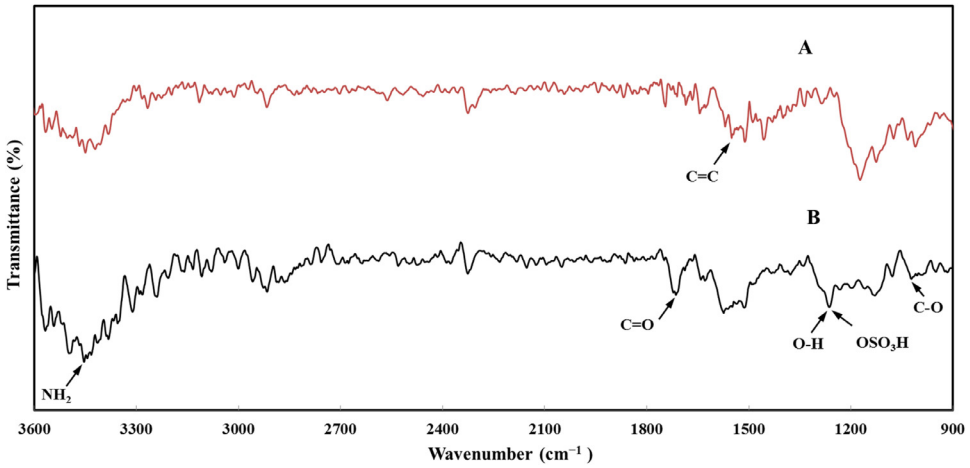

Fig. 3. The FTIR spectra of (A) Raw MWCNTs and (B) Functionalized MWCNTs.

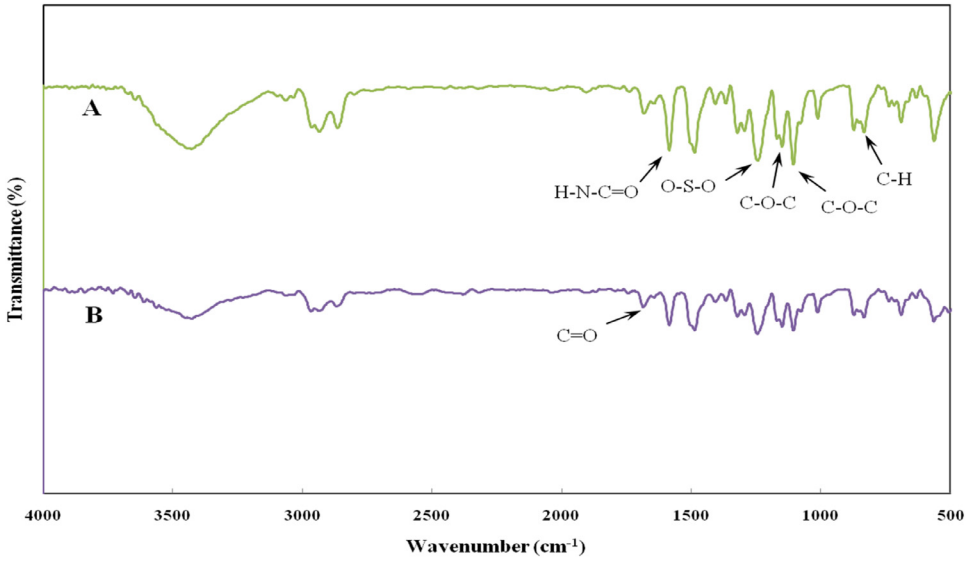

Fig. 4. The FT-IR spectra of (A) PSf/Pebax and (B) PSf/Pebax/F-MWCNT membranes.

of raw and modified MWCNTs is demonstrated in Fig. 3. As observed from FTIR spectrum of Fig. 3B, the new peaks emerging at 1021, 1258 and 1715 cm^{-1} after the functionalization of MWCNTs corresponds to C–O, OSO_3H and O–H and C=O bonds, respectively [15,16]. The band at 1580 cm^{-1} is likely due to conjugation of C=O with C=C bonds or interaction between localized C=C bonds and carboxylic acids [15,17]. Moreover, the new peak at 3498 cm^{-1} corresponds to $-NH_2$ groups [18,19]. This confirms the attachment of the functional groups onto the MWCNTs. The hydrophilic properties of the functional groups improve the dispersibility of F-MWCNTs in aqueous solution.

3.2. Characterization of prepared membranes

Fig. 4 exhibits the FTIR spectra of the PSf/pebax membrane and the PSf/pebax/F-MWCNT membrane. As can be seen in Fig. 4A bands at 1110 and 1640 cm^{-1} corresponded to C–O–C and H–N–C=O in pebax polymer, respectively [20]. Also, absorption bands at 812, 1151 and 1244 cm^{-1} related to C–H, C–O–C and O-S-O in PSf polymer, respectively [21–24]. According to Fig. 3, the functionalized MWCNTs exhibited three main bands: 1021 (C–O), 1258 (OSO_3H) and 1715 cm^{-1} (–C=O). The FTIR spectrum of the blend membrane (Fig. 4B) depicts the same peaks at 1715 cm^{-1}. Appearance of this peak approves the presence of F-MWCNTs in the surface of the membrane. Similar results were obtained by Choi et al. [25].

Table 2
Water contact angle for prepared membranes.

Membrane	Contact angle (°)
PSf/pebax	55.1 ± 0.63
PSf/pebax/0.5%F-MWCNT	50.6 ± 0.44
PSf/pebax/1%F-MWCNT	45.3 ± 0.96
PSf/pebax/2%F-MWCNT	42.5 ± 0.28

3.3. Water contact angle

The hydrophilicity of PSf/pebax/F-MWCNT membrane surfaces was characterized by water contact angle. As shown in Table 2, when F-MWCNTs loading were increased, the contact angles of the membranes gradually declined which means hydrophilicity increases. The PSf/pebax membrane had the highest water contact angle of 55.1 ± 0.63° while water contact angel of PSf/pebax/1%F-MWCNT reached 45.3 ± 0.96° and decreased about 10° This indicated that F-MWCNT membranes possessed lower water contact angles, which implies the hydrophilicity of membranes is improved with an increase of F-MWCNT amount [18]. As can be seen in

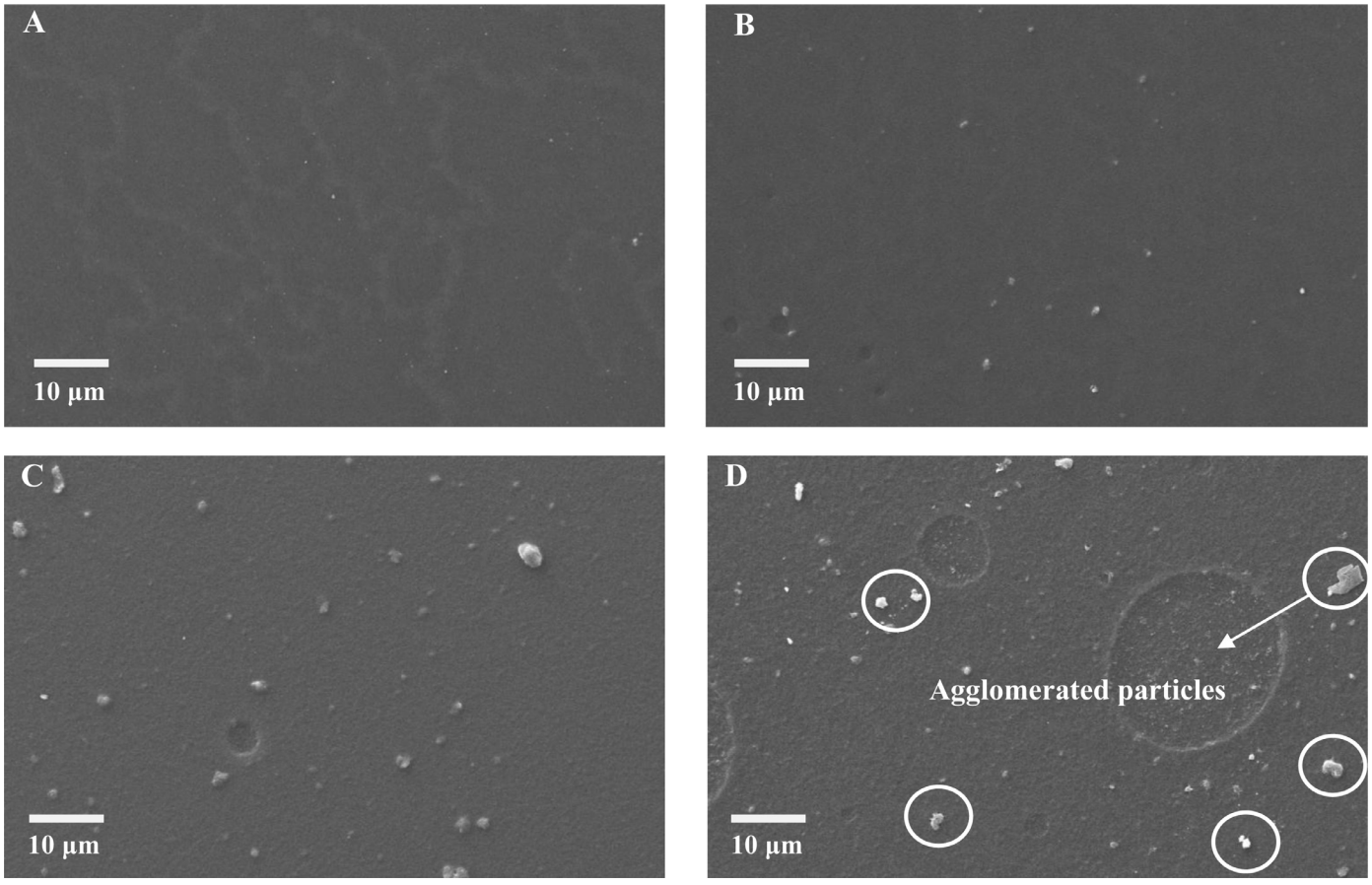

Fig. 5. Surface SEM images of PSf/pebax nanocomposite membranes prepared with different F-MWCNTs loading: (A) 0.0 wt%, (B) 0.5 wt%, (C) 1 wt% and (D) 2 wt%.

Table 2, increasing the F-MWCNT amount to more than 2 wt% did not result in remarkable enhancement of the hydrophilicity, and the water contact angel value of PSf/pebax/2%F-MWCNT membrane was 42.5 ± 0.28° This behavior for MWCNT/polyethersulfone membrane was also previously reported [12]. This might be explained by the irregular positioning of F-MWCNTs in the membrane structure at over 1 wt% MWCNT content, which leads to aggregation and reducing effective surface of nanotubes [17,26].

3.4. SEM

Surface SEM images of composite membranes with different F-MWCNTs loading are presented in Fig. 5. Obviously, the PSf/pebax membrane was free of F-MWCNTs particles, and increasing the loading of F-MWCNTs increased the number of light spots, which illustrate the F-MWCNTs [27]. As observed in Fig. 5, F-MWCNTs particles were not agglomerated and were distributed very well along the surface of the membrane at 0.5 wt% [28]. Also, there was not any noticeable agglomeration of F-MWCNTs in this membrane compared to the nanocomposite membrane prepared with 1 and 2 wt% F-MWCNT, as can be observed in Fig. 5C and D [29]. Panahian et al. [30] prepared multilayer mixed matrix membrane containing CNTs, PVA, PES and polyester as inorganic filler and selective top, intermediate and support layers, respectively. They reported that some bright spots on the surface of the membrane samples containing CNTs can be seen from SEM images. Moreover, the SEM image on the membrane containing 4 wt% CNTs indicated that the MWCNTs are agglomerated.

The pebax solution containing F-MWCNTs was cast on a PSf UF membrane that was coated on woven polyester. Cross-sectional SEM images of the membranes prepared with 0 and 2% loading of F-MWCNTs are presented in Fig. 6. The PSf support provides a suitable porosity and excellent mechanical strength for casting the pebax selective layer. Similar observations was reported about PVDF/PVA/MWCNT nanocomposite membranes with two distinct layers depicting the PVA–MWCNTs layer being coated on the PVDF membrane [31].

As observed in Fig. 6, there was good compatibility between the pebax selective layer and the PSf UF support, and the thickness of the pebax selective layer was around 1–2 μm. Khan et al. [29] prepared a nanocomposite membrane by dispersion different loading of F-MWCNTs within polymers of intrinsic microporosity (PIM-1) matrix and the PAN microporous membrane used as a support. They observed that the average thickness of selective layer of all membranes was about 0.75 μm. The cross section images of F-MWCNTs MMM indicated that most of the functionalized MWCNTs were well dispersed in PIM-1 matrix and there was also no evidence of interfacial voids in the prepared membrane.

As seen in Fig. 6, there was no sign of agglomeration, interface voids, or sieving in the cage morphology of the prepared membranes. This good affinity between the polymer matrix and the F-MWCNT particles is owed to the presence of the functional groups in MWCNTs. Good distribution of MWCNTs particles within polymer matrix was due to functional groups which can be observed in other studies [27,28]. There was also no evidence of interface voids or sieve in cage morphology of these membranes.

3.5. Tensile strength

The tensile strength at the break of the PSf/pebax and the PSf/pebax/F-MWCNT membranes were determined to study the impact of adding F-MWCNTs on the mechanical strengths of

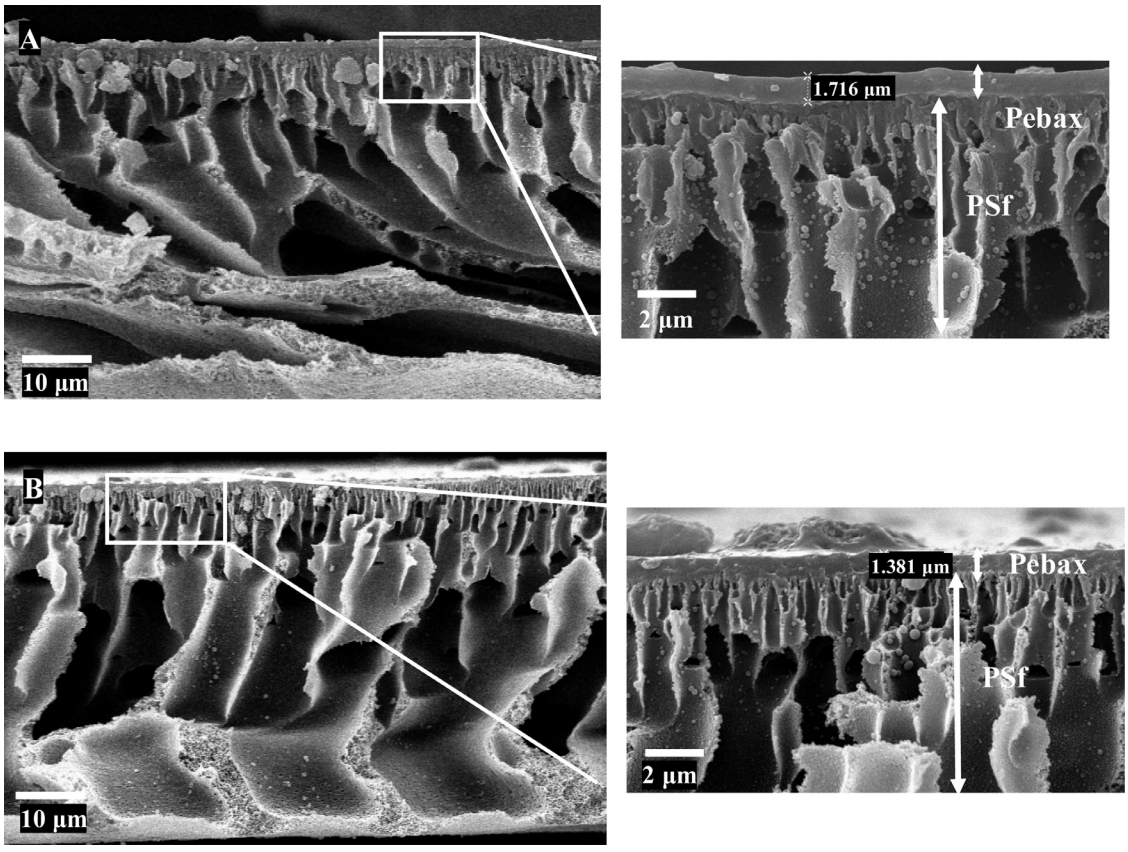

Fig. 6. Cross-sectional SEM images of PSf/pebax nanocomposite membranes prepared with F-MWCNTs loading: (A) 0.0 wt%, (B) 2 wt%.

Table 3
Effect of F-MWCNTs on the mechanical stability of nanocomposite membranes.

Membrane	PSf/pebax	PSf/pebax/0.5%F-MWCNT	PSf/pebax/1%F-MWCNT	PSf/pebax/2%F-MWCNT
Tensile strength at break (MPa)	1.25 ± 0.21	2.27 ± 0.16	2.72 ± 0.23	2.68 ± 0.19

membranes. This test was carried out for all samples. Each test was repeated three times for each sample and mean values are presented in Table 3. Considering the obtained data, it can be said that the tensile strength of the polymer matrix is promoted by the addition of F-MWCNTs compared to PSf/Pebax, while further increase of F-MWCNTs lead to reduction in tensile strength of nanocomposite membranes. The increase in tensile strength implies the well dispersion of F-MWCNTs among the polymer matrix and strong interaction between pebax and functionalized MWCNTs. The functionalized MWCNTs contain many defects and hydrophilic groups, such as -OH and -COOH, so a strong hydrogen-bond may be formed between pebax and the F-MWCNTs. Besides, high amount of F-MWCNTs has negatively affected the mechanical properties of membranes due to agglomeration of F-MWCNTs [32]. These variations in tensile strength of membranes are consistent with FTIR and SEM results saying that well dispersion of F-MWCNTs among the polymer matrix can be achieved only in low F-MWCNTs loading.

3.6. TGA

The effect of F-MWCNTs on the thermal stability of prepared membranes was studied using TGA. As shown in Figs. 7 and 8, the weight reduction of membranes takes place in five steps. The first step of weight loss occurred in the temperature range from 120 to 214 °C is related to the evaporation of residual solvent and moisture. The second step of weight loss for PSf/pebax membrane begins at 214 °C which is attributed to decomposition of pebax polymer chains [33]. In the third step, decomposition of interface polymer chains between pebax and PSf layers is occurred at 420 °C. The fourth step of weight loss starts at 520 °C which is attributed to decomposition of PSf polymer chains [34]. Finally, at the fifth step total degradation of samples occurs at 598 °C. TGA curve of nanocomposite membrane obeys the same behavior. Table 4 summarizes the TGA results of nanocomposite membranes. As can be seen, second and third decomposition temperature of nanocomposite membrane is higher than that of PSf/pebax membrane. As mentioned before, well dispersion of F-MWCNTs among the polymer matrix and strong hydrogen-bond between pebax and the F-MWCNTs enhances its thermal stability. Therefore, more energy is required to disrupt chains. Similar results can be found in the literature which is consistent with our study. For example, Mansourpanah et al. [35] and Phao et al. [36] reported that addition of F-MWCNT to PES membrane enhances its thermal stability significantly. Also Murthy et al. [37] observed that by addition of F-MWCNT in chitosan matrix, thermal stability of prepared membranes improved about 120 °C.

3.7. Oil/water nanofiltration experiments

3.7.1. Effect of transmembrane pressure (TMP) on permeate flux

Fig. 9 shows the variations of permeate flux at TMP from 10 to 20 bar for PSf/Pebax nanocomposite membranes prepared with different F-MWCNTs loading. The steady permeate flux was highly

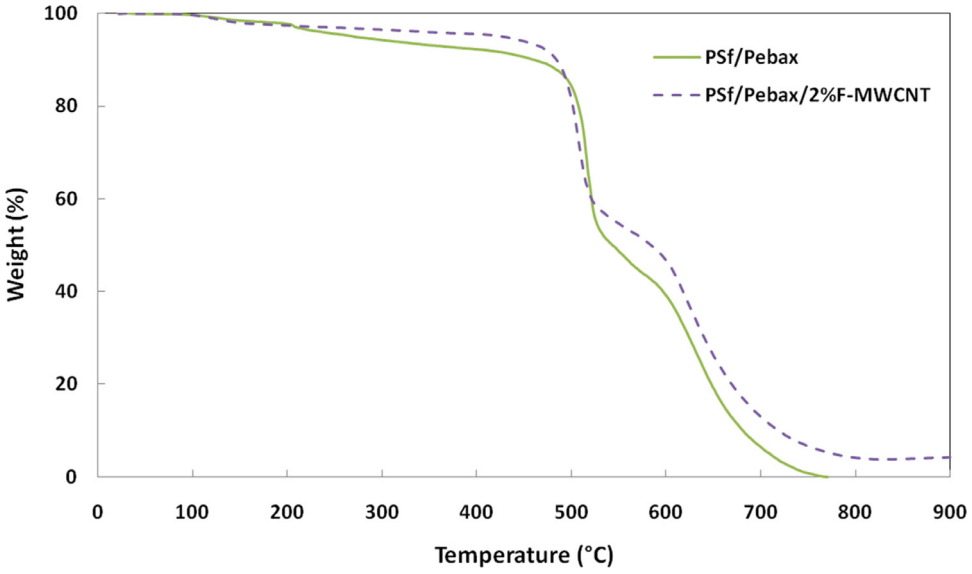

Fig 7. Thermogravimetric analysis of PSf/pebax and PSf/pebax/F-MWCNT membranes.

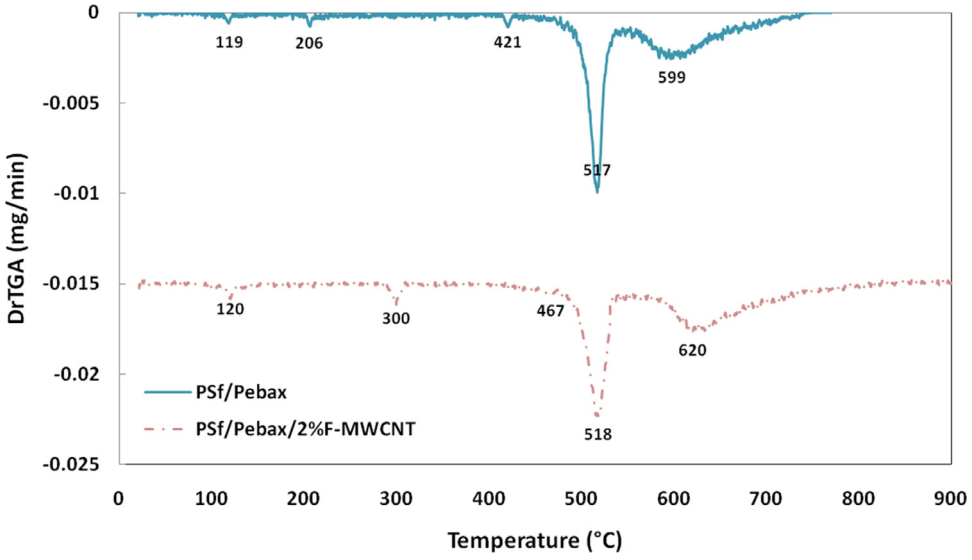

Fig 8. Derivative thermogravimetric analysis of PSf/pebax and PSf/pebax/F-MWCNT membranes.

Table 4
TGA results of nanocomposite membranes.

Membrane	First decomposition temperature (°C)	Second decomposition temperature (°C)	Third decomposition temperature (°C)	Fourth decomposition temperature (°C)	Fifth decomposition temperature (°C)
PSf/pebax	119	206	421	517	599
PSf/pebax/2%F-MWCNT	120	300	467	518	620

dependent on TMP. It was also found that the increase of permeate flux under lower TMP was greater than that under higher TMP. When the TMP was greater than 15 bar, the rate of increase of permeate flux was reduced. This is because the increase of TMP had both positive and negative effects on the permeate flux. Higher TMP allowed droplets (both solvent and solute) to pass rapidly through the membrane pores. However, more oil droplets accumulated both on the membrane surface and in the membrane pores, leading to membrane fouling [38]. According to Fig. 9, the positive effect on the permeate flux was predominant at low TMP levels. Beyond the threshold pressure, the flux increases slowly with TMP due to membrane fouling [39,40].

3.7.2. Effect of F-MWCNTs on permeate flux

As can be seen in Fig. 9, addition of F-MWCNT to PSf/Pebax membrane leads to increase in permeate flux up to 0.5 wt% of F-MWCNT while permeate flux reduced by further increase of F-MWCNT loading in polymer matrix. The permeate flux of membranes is usually controlled by two factors; hydrophilicity and the porosity of the membrane [17]. The hydrophilic groups of F-MWCNTs surface improve the hydrophilicity of membrane surface (see Table 2). This increase in hydrophilicity results in an increase in permeate flux. In addition, the increase in porosity leads to increasing permeate flux through the membranes. Increasing water flux up to 0.5 wt% of F-MWCNT loading can be attributed to

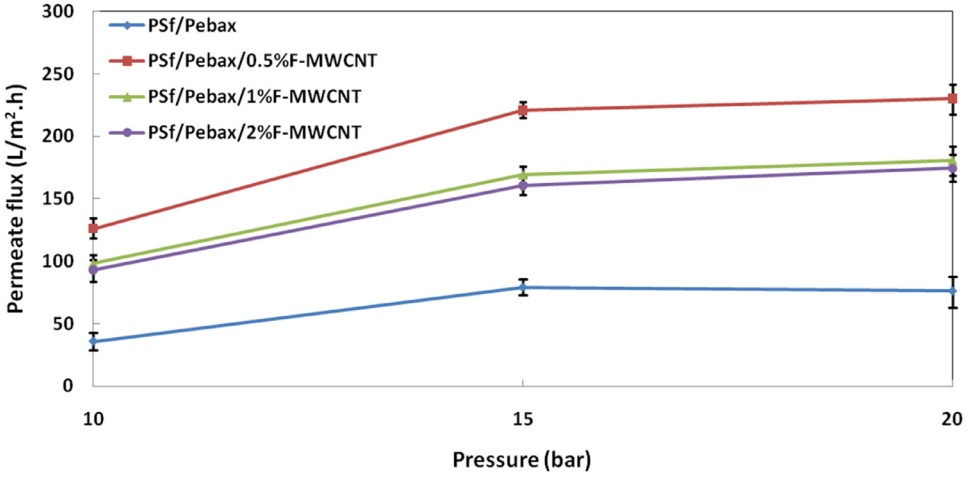

Fig. 9. Effect of TMP on permeate flux of PSf/Pebax nanocomposite membranes prepared with different contents of F-MWCNTs.

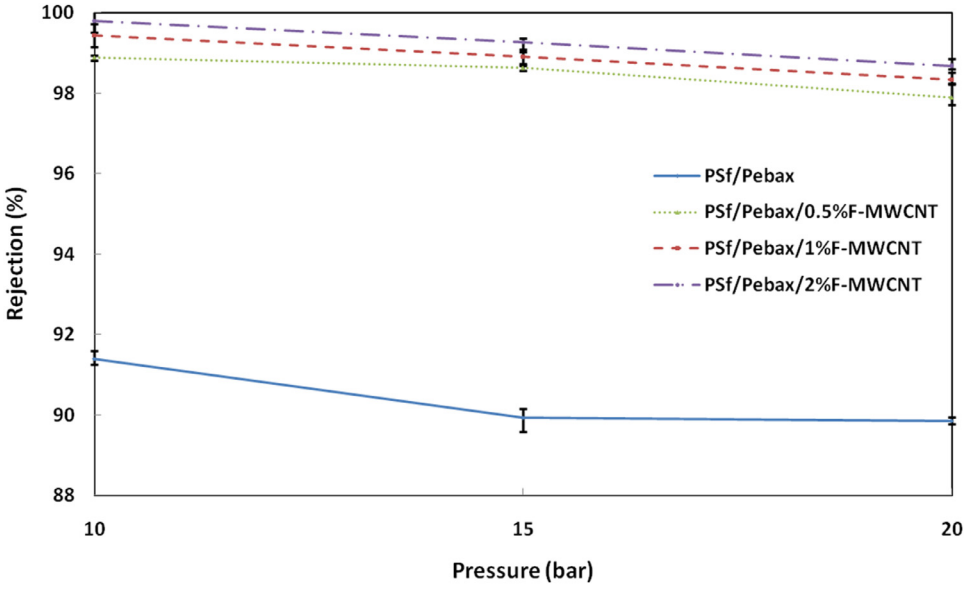

Fig. 10. Effect of TMP on oil rejection of PSf/Pebax nanocomposite membranes prepared with different contents of F-MWCNTs.

improvement of membrane hydrophilicity due to functional groups of F-MWCNTs and increase of the porosity causing the more solvent evaporation from polymer solution during phase separation. However, when the F-MWCNTs loading exceeds 0.5 wt%, the high density of F-MWCNTs leads to an increase in the viscosity of casting solution. This will hinder the solvent evaporation from polymer solution. Also, the density of F-MWCNTs in the membrane is so large that the steric hindrance and electrostatic interactions among the F-MWCNTs and between the F-MWCNTs and the polymer chains cause to cluster the F-MWCNTs during membrane preparation. Therefore, a less porous membrane is created and the flux decreases. Choi et al. [25] obtained similar results by adding F-MWCNT to PSf ultrafiltration membrane. They observed that the pore size and permeation of the blend membranes increased with adding of F-MWCNTs up to 1.5% and then decreased because of increasing in the viscosity of casting solution.

3.7.3. Effect of TMP on oil rejection

The variation in oil rejection for prepared membranes at different TMP is presented in Fig. 10. From the figure, it is found that at lower pressure range, the rejection is more; while at higher pressure, the rejection shows a decreasing trend. This is because of the fact that higher pressure drop across the membrane would enhance wetting and coalescence of the oil droplets by increasing convection and this would impose some oil droplets to pass through the membrane pores along with the permeate. In other words, as the transmembrane pressure increases, the applied pressure overcomes the capillary pressure that prevents the oil from entering the membrane pores [41–43]. Consequently, J_{oil} increases more than J_w by increasing pressure and $C_p = J_{oil}/J_w$ increases; therefore according to Eq. (2), oil rejection decreases.

3.7.4. Effect of F-MWCNTs on oil rejection

Effect of F-MWCNTs loading on oil rejection of prepared membranes at different TMP is shown at Fig. 10. By incorporation of F-MWCNT into pebax matrix, oil rejection is improved. As can be seen, oil rejection at TMP of 10 bar for PSf/Pebax membrane is 91.40% and for PSf/Pebax/2%F-MWCNT membrane is 99.79%, which is about 8% higher. The rejection behavior in the nanocomposite membranes might be explained by a combination of two effects. First, the increment in hydrophilicity due to addition of F-MWCNTs enhances the permeation of water through the membrane. This affects the rejection positively by increasing the total amount of water molecules that permeates through the

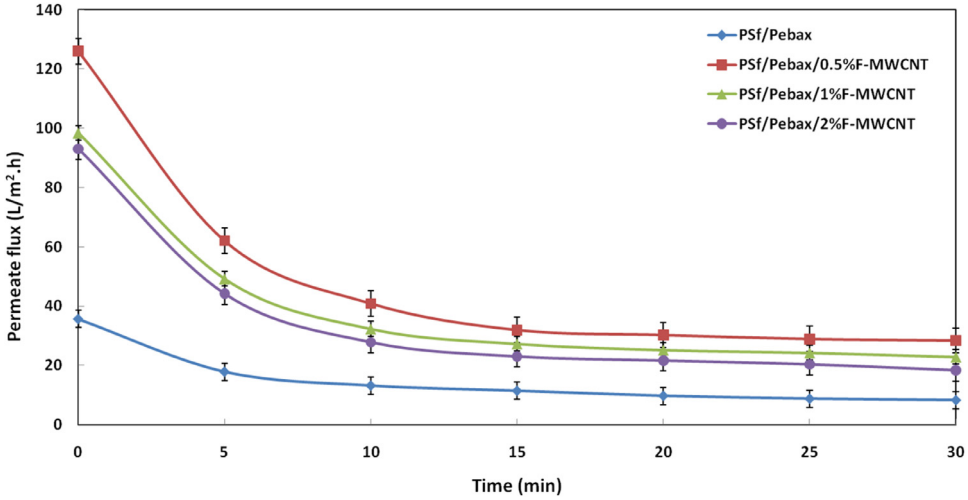

Fig. 11. Flux declines of the prepared nanocomposite membranes at TMP of 10 bar

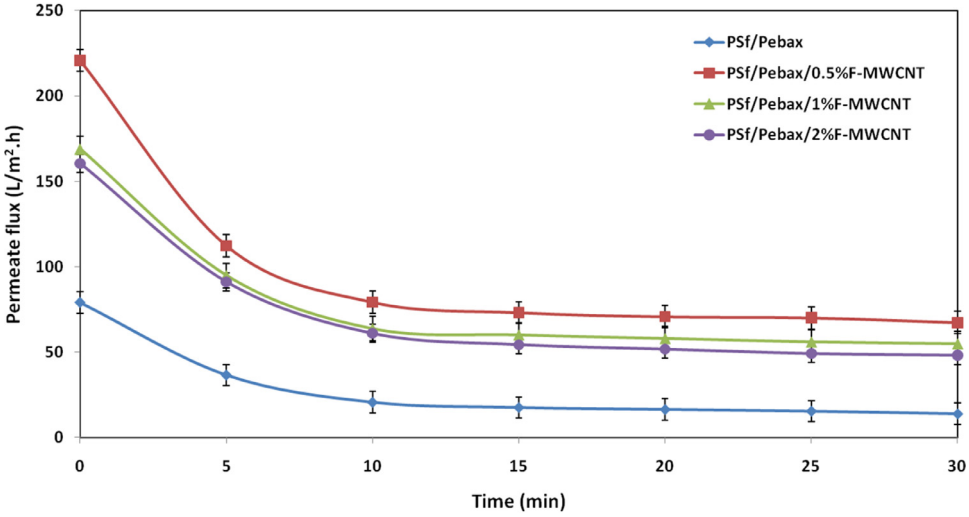

Fig. 12. Flux declines of the prepared nanocomposite membranes at TMP of 15 bar

membrane without enhancing the permeability of oil. Second, reduction of membrane porosity and smaller pores when the F-MWCNTs loading exceeds 0.5 wt% leads to increase in oil rejection of PSf/Pebax/1%F-MWCNT and PSf/Pebax/2%F-MWCNT membranes compared to PSf/Pebax/0.5%F-MWCNT membrane.

3.8. Antifouling and recycling properties of the membranes

3.8.1. Flux decline

Figs. 11–13 show flux decline for prepared membranes at various TMP during NF of the O/W emulsion. As observed, the variation of permeate flux can be divided into two stages, a sharp decay and a pseudo-steady stage. At the early period of filtration, the flux reduces very quickly due to the rapid membrane blocking and fouling. The reduction rate in permeate flux becomes very slow after 15 min. In fact, the permeate fluxes approach to their pseudo-steady values [44].

3.8.2. Antifouling properties

To investigate the pressure effect on flux decline, flux decline at different TMP versus time for PSf/Pebax/2%F-MWCNT is presented in Fig. 14. The rate of flux decline is greater at high pressure as can be seen in Fig. 14. It can be attributed to the build-up of the concentration polarization layer and pore blocking mechanisms which was also observed by Chakrabarty et al. [9]. Increase in pressure increases the number of collisions between the emulsion droplets, which in turn break the film between the oil and water causing the oil droplets to coalesce and form large droplets. As a result, a layer containing large oil droplets starts forming just above the membrane surface which may be compressed on the surface at higher pressure leading to membrane fouling at a higher rate. This phenomenon declines the flux. However at each pressure, for all the membranes, the permeation flux is seen to reach almost a constant value after 15 min.

The antifouling performance of the PSf/Pebax and PSf/Pebax/F-MWCNT nanofiltration membranes was characterized by means of measuring water flux recovery after fouling by O/W emulsion. The results are shown in Table 5. From the table, it is clear that the flux recovery percentage of the F-MWCNT embedded membranes is higher than that of the PSf/Pebax membrane. It means that the filtration performance of the nanocomposite membranes was enhanced when they were exposed to O/W emulsion. The flux recovery value of PSf/Pebax membrane was only 73.29% implicating a poor antifouling property. In the best case, the flux recovery percentage of the 2 wt% F-MWCNT membrane was 97.79%.

The adsorption and deposition of oil droplets on the membrane surface and their entrapment in the pores primarily caused membrane fouling. Membrane fouling consisted of reversible fouling

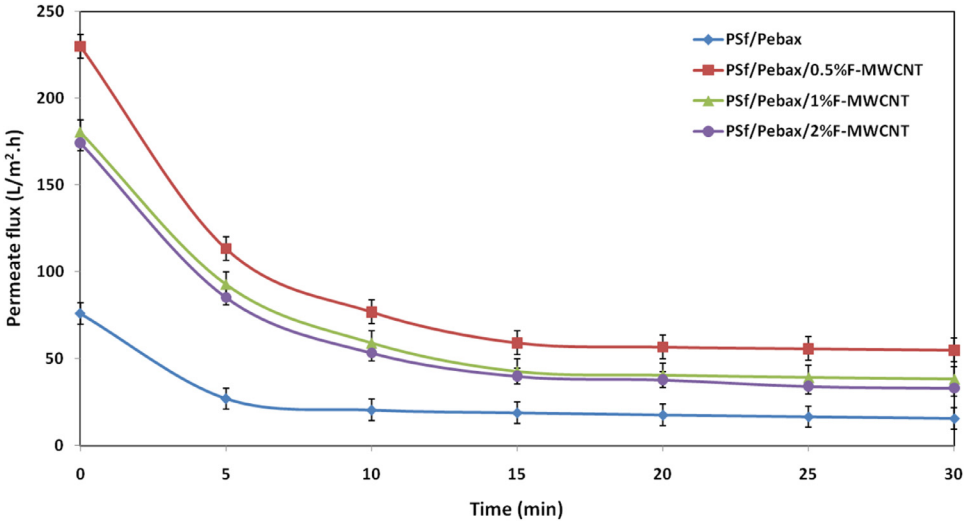

Fig. 13. Flux declines of the prepared nanocomposite membranes at TMP of 20 bar

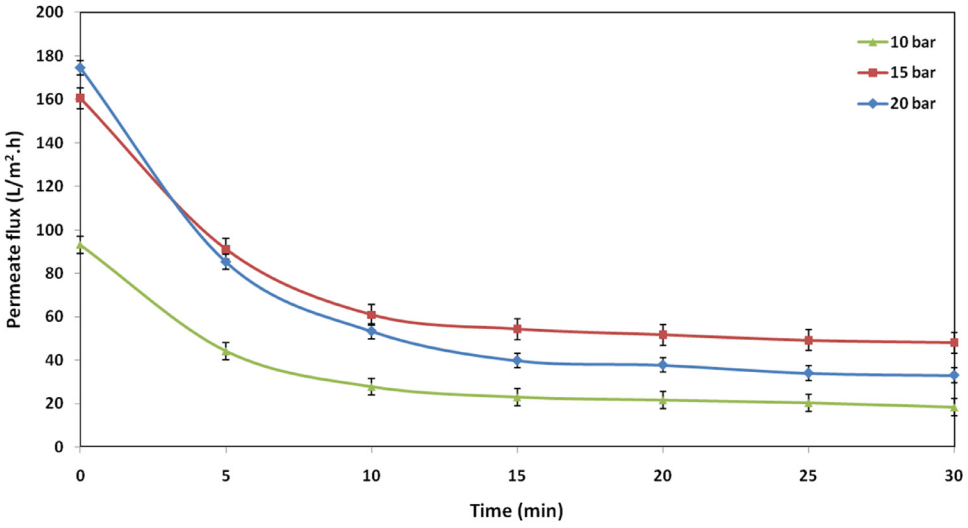

Fig. 14. Flux decline of PSf/pebax/2%F-MWCNT membrane at various TMP.

Table 5
Flux recovery, irreversible and reversible deposition on membrane surfaces.

Membrane	*FRR* (%)			R_{ir} (%)			R_r (%)		
	Pressure (bar)			Pressure (bar)			Pressure (bar)		
	10	15	20	10	15	20	10	15	20
PSf/pebax	90.15	89.79	73.29	9.85	10.21	26.71	12.04	9.19	8.90
PSf/pebax/0.5%FMWCNT	96.71	96.10	90.80	3.29	3.90	9.20	13.82	9.95	9.38
PSf/pebax/1%F-MWCNT	97.48	96.68	91.61	2.52	3.32	8.39	14.71	10.23	9.75
PSf/pebax/2%F-MWCNT	97.79	97.61	91.95	2.21	2.39	8.05	15.47	12.46	11.73

and irreversible fouling. Reversible oil droplets adsorption led to reversible fouling which could be removed by simple hydraulic cleaning. On the contrary, irreversible fouling was caused by firm adsorption of oil droplets on the surface or entrapment of oil droplets inside pores [43,60], 60]. Table 5 also shows reversible fouling ratio (R_r), and irreversible fouling ratio (R_{ir}) values which calculated from water flux before O/W separation and after hydraulic cleaning to evaluate the antifouling properties. Reversible fouling of PSf/Pebax and F-MWCNT modified PSf/Pebax membranes roughly was similar. However, the main difference in fouling resistance of membranes was observed in irreversible fouling value. This implies the irreversible fouling dominates the total fouling. PSf/Pebax membrane had high irreversible fouling due to its lower hydrophilicity. Among the F-MWCNT blended membranes, 2 wt% membrane represented lowest irreversible fouling, which can be attributed to its higher hydrophilicity (Table 2).

Obviously, finding identical conditions including TMP, membrane material and separation process in literature is impossible. Therefore, the efficiency of different membranes used in separation of O/W emulsion compared to present study, despite the different conditions and different membrane processes (UF and NF). As it can be seen in Table 6, the permeate flux of the

Table 6
The O/W separation performance of different membrane processes.

Membrane	Membrane process	Additive	TMP (bar)	Flux (L/m^2 h)	R% (%)	Ref.
Felt-metal supported PVA composite	UF	–	4.5	113	92.7	[38]
TFC polyamide commercial	NF	–	5	47	82	[43]
PSf	UF	PVP & PEG	1	82	97	[6]
PVDF	UF	PEG400 & PEG15000	1.5	11.55	98	[44]
γ-Al_2O_3	NF	–	10	44	96.3	[5]
PSA & PEA	NF	PVP	20	5	99.16	[4]
PSf commercial	UF	–	3	100	80	[39]
TFN polyamide commercial	NF	–	10	80	92	[3]
PSf/pebax	NF	0.5%F-MWCNT	15	230	98.63	This study
PSf/pebax	NF	2%F-MWCNT	15	174.4	99.26	This study

PSf/Pebax/0.5%F-MWCNT membrane (230 L/m^2 h) prepared in the present study is higher than those of most membranes reported in the literature for O/W separation. Moreover, PSf/Pebax/2%F-MWCNT membrane has relatively higher oil rejection value (99.26%) in comparison to other studies.

4. Conclusions

A new PSf/Pebax nanofiltration composite membrane was successfully prepared, modified and characterized. To modify the characteristics of the resulting membrane, 0.5, 1 and 2 wt% of F-MWCNT were added to pebax solution. The stabilization of F-MWCNTs in membrane matrix approved by FTIR. The surface of membranes was nearly smooth and defect free. A dense pebax layer was formed on the porous PSf layer and there was no evidence of interface voids or sieve in cage morphology of these membranes. Increasing F-MWCNT, decreases water contact angel and consequently increases membrane hydrophilicity. Tensile strength of membrane was increased by addition of F-MWCNT. Furthermore, adding F-MWCNT to polymer matrix enhances thermal stability of membrane. Increasing F-MWCNT content up to 0.5 wt%, increases permeate flux and further increasing of F-MWCNT to 2 wt%, decreases permeate flux. Rejection of oil/water emulsion is higher at lower pressure while by increasing pressure; rejection has a decreasing trend, and oil rejection increases with increasing F-MWCNT loading.

Acknowledgments

The authors acknowledge Iran Nanotechnology Initiative Council for financial support.

References

[1] Coca J, Gutiérrez G, Benito J. Treatment of oily wastewater. Water Purif Manag. Springer; 2011. p. 1–55.
[2] Li B, Zhang J, Gao Z, Wei Q. Semitransparent superoleophobic coatings with low sliding angles for hot liquids based on silica nanotubes. J Mater Chem A 2016;4:953–60.
[3] Zhang J, Seeger S. Polyester materials with superwetting silicone nanofilaments for oil/water separation and selective oil absorption. Adv Funct Mater 2011;21:4699–704.
[4] Li L, Li B, Wu L, Zhao X, Zhang J. Magnetic, superhydrophobic and durable silicone sponges and their applications in removal of organic pollutants from water. Chem Commun 2014;50:7831–3.
[5] Park E, Barnett SM. Oil/water separation using nanofiltration membrane technology. Sep Sci Technol 2001;36:1527–42.
[6] Panpanit S, Visvanathan C, Muttamara S. Separation of oil-water emulsion from car washes. Water Sci Technol 2000;41:109–16.
[7] Chan WH, Tsao SC. Preparation and characterization of nanofiltration membranes fabricated from poly (amidesulfonamide), and their application in water–oil separation. J Appl Polym Sci 2003;87:1803–10.
[8] Sadeghian Z, Zamani F, Ashrafizadeh S. Removal of oily hydrocarbon contaminants from wastewater by γ-alumina nanofiltration membranes. Desalin Water Treat 2010;20:80–5.
[9] Chakrabarty B, Ghoshal A, Purkait M. Ultrafiltration of stable oil-in-water emulsion by polysulfone membrane. J Membr Sci 2008;325:427–37.
[10] Su Y-L, Cheng W, Li C, Jiang Z. Preparation of antifouling ultrafiltration membranes with poly (ethylene glycol)-graft-polyacrylonitrile copolymers. J Membr Sci 2009;329:246–52.
[11] Wu T, Pan Y, Li L. Fabrication of superhydrophobic hybrids from multiwalled carbon nanotubes and poly (vinylidene fluoride). Colloids Surf A: Physicochem Eng ASP 2011;384:47–52.
[12] Celik E, Park H, Choi H, Choi H. Carbon nanotube blended polyethersulfone membranes for fouling control in water treatment. Water Res 2011;45:274–82.
[13] Majeed S, Fierro D, Buhr K, Wind J, Du B, Boschetti-de-Fierro A, et al. Multi-walled carbon nanotubes (MWCNTs) mixed polyacrylonitrile (PAN) ultrafiltration membranes. J Membr Sci 2012;403:101–9.
[14] Wu H, Tang B, Wu P. Novel ultrafiltration membranes prepared from a multi-walled carbon nanotubes/polymer composite. J Membr Sci 2010;362:374–83.
[15] Vuković GD, Marinković AD, Čolić M, Ristić MĐ, Aleksić R, Perić-Grujić AA, et al. Removal of cadmium from aqueous solutions by oxidized and ethylenediamine-functionalized multi-walled carbon nanotubes. Chem Eng J 2010;157:238–48.
[16] Yu R, Chen L, Liu Q, Lin J, Tan K-L, Ng SC, et al. Platinum deposition on carbon nanotubes via chemical modification. Chem Mater 1998;10:718–22.
[17] Vatanpour V, Madaeni SS, Moradian R, Zinadini S, Astinchap B. Fabrication and characterization of novel antifouling nanofiltration membrane prepared from oxidized multiwalled carbon nanotube/polyethersulfone nanocomposite. J Membr Sci 2011;375:284–94.
[18] Ma J, Zhao Y, Xu Z, Min C, Zhou B, Li Y, et al. Role of oxygen-containing groups on MWCNTs in enhanced separation and permeability performance for PVDF hybrid ultrafiltration membranes. Desalination 2013;320:1–9.
[19] Rahimpour A, Jahanshahi M, Khalili S, Mollahosseini A, Zirepour A, Rajaeian B. Novel functionalized carbon nanotubes for improving the surface properties and performance of polyethersulfone (PES) membrane. Desalination 2012;286:99–107.
[20] Liu S, Liu G, Zhao X, Jin W. Hydrophobic-ZIF-71 filled PEBA mixed matrix membranes for recovery of biobutanol via pervaporation. J Membr Sci 2013;446:181–8.
[21] Panda SR, De S. Preparation, characterization and performance of $ZnCl_2$ incorporated polysulfone (PSF)/polyethylene glycol (PEG) blend low pressure nanofiltration membranes. Desalination 2014;347:52–65.
[22] Song YQ, Sheng J, Wei M, Yuan XB. Surface modification of polysulfone membranes by low-temperature plasma–graft poly (ethylene glycol) onto polysulfone membranes. J Appl Polymer Sci 2000;78:979–85.
[23] Pakizeh M, Moghadam AN, Omidkhah MR, Namvar-Mahboub M. Preparation and characterization of dimethyldichlorosilane modified SiO_2/PSf nanocomposite membrane. Korean J Chem Eng 2013;30:751–60.
[24] Sinha M, Purkait M. Preparation of fouling resistant PSF flat sheet UF membrane using amphiphilic polyurethane macromolecules. Desalination 2015;355:155–68.
[25] Choi J-H, Jegal J, Kim W-N. Fabrication and characterization of multi-walled carbon nanotubes/polymer blend membranes. J Membr Sci 2006;284:406–15.
[26] Qiu S, Wu L, Pan X, Zhang L, Chen H, Gao C. Preparation and properties of functionalized carbon nanotube/PSF blend ultrafiltration membranes. J Membr Sci 2009;342:165–72.
[27] Amirilargani M, Tofighy MA, Mohammadi T, Sadatnia B. Novel poly (vinyl alcohol)/Multiwalled carbon nanotube nanocomposite membranes for pervaporation dehydration of isopropanol: poly (sodium 4-styrenesulfonate) as a functionalization agent. Ind Eng Chem Res 2014;53:12819–29.
[28] Amirilargani M, Ghadimi A, Tofighy MA, Mohammadi T. Effects of poly (allylamine hydrochloride) as a new functionalization agent for preparation of poly vinyl alcohol/multiwalled carbon nanotubes membranes. J Membr Sci 2013;447:315–24.
[29] Khan MM, Filiz V, Bengtson G, Shishatskiy S, Rahman M, Abetz V. Functionalized carbon nanotubes mixed matrix membranes of polymers of intrinsic microporosity for gas separation. Nanoscale Res Lett 2012;7:1–12.
[30] Panahian S, Raisi A, Aroujalian A. Multilayer mixed matrix membranes containing modified-MWCNTs for dehydration of alcohol by pervaporation process. Desalination 2015;355:45–55.
[31] Yeang QW, Zein SHS, Sulong AB, Tan SH. Comparison of the pervaporation performance of various types of carbon nanotube-based nanocomposites in the dehydration of acetone. Sep Purif Technol 2013;107:252–63.

[32] O'Connor I, Hayden H, O'Connor S, Coleman JN, Gun'ko YK. Kevlar coated carbon nanotubes for reinforcement of polyvinylchloride. J Mater Chem 2008;18:5585–8.
[33] José Cirilo Ignacio L-E, Ant L, Karl S, Emilio B. PEBAX™-silanized Al_2O_3 composite, synthesis and characterization. Open J Polym Chem 2012;2012.
[34] Momeni S, Pakizeh M. Preparation, characterization and gas permeation study of PSf/MgO nanocomposite membrane. Braz J Chem Eng 2013;30:589–97.
[35] Mansourpanah Y, Madaeni S, Rahimpour A, Adeli M, Hashemi M, Moradian M. Fabrication new PES-based mixed matrix nanocomposite membranes using polycaprolactone modified carbon nanotubes as the additive: property changes and morphological studies. Desalination 2011;277:171–7.
[36] Phao N, Nxumalo EN, Mamba BB, Mhlanga SD. A nitrogen-doped carbon nanotube enhanced polyethersulfone membrane system for water treatment. Phys Chem Earth, Parts A/B/C 2013;66:148–56.
[37] Murthy Z, Gaikwad MS. Preparation of chitosan-multiwalled carbon nanotubes blended membranes: characterization and performance in the separation of sodium and magnesium ions. Nanoscale Microscale Thermophys Eng 2013;17:245–62.
[38] Hua FL, Tsang YF, Wang YJ, Chan SY, Chua H, Sin SN. Performance study of ceramic microfiltration membrane for oily wastewater treatment. Chem Eng J 2007;128:169–75.
[39] Chang Q, Zhou J-e, Wang Y, Liang J, Zhang X, Cerneaux S, et al. Application of ceramic microfiltration membrane modified by nano-TiO_2 coating in separation of a stable oil-in-water emulsion. J Membr Sci 2014;456:128–33.
[40] Qiu Y-R, Zhong H, Zhang Q-X. Treatment of stable oil/water emulsion by novel felt-metal supported PVA composite hydrophilic membrane using cross flow ultrafiltration. Trans Nonferrous Met Soc China 2009;19:773–7.
[41] Madaeni S, Gheshlaghi A, Rekabdar F. Membrane treatment of oily wastewater from refinery processes. Asia-Pac J Chem Eng 2013;8:45–53.
[42] Emani S, Uppaluri R, Purkait MK. Microfiltration of oil–water emulsions using low cost ceramic membranes prepared with the uniaxial dry compaction method. Ceram Int 2014;40:1155–64.
[43] Chakrabarty B, Ghoshal AK, Purkait MK. Ultrafiltration of stable oil-in-water emulsion by polysulfone membrane. J Membr Sci 2008;325:427–37.
[44] Salahi A, Abbasi M, Mohammadi T. Permeate flux decline during UF of oily wastewater: experimental and modeling. Desalination 2010;251:153–60.